NASA Technical Memorandum 79135

PRELIMINARY RESULTS IN THE NASA LEWIS H_2-O_2 COMBUSTION MHD EXPERIMENT

J. Marlin Smith
Lewis Research Center
Cleveland, Ohio

Prepared for the
Eighteenth Symposium on the Engineering Aspects
of Magnetohydrodynamics
Butte, Montana, June 18-20, 1979

PRELIMINARY RESULTS IN THE NASA LEWIS H_2-O_2 COMBUSTION MHD EXPERIMENT

J. Marlin Smith
NASA Lewis Research Center
Cleveland, Ohio 44135

Abstract

MHD power generation experiments have been carried out in the NASA Lewis Research Center cesium-seeded H_2-O_2 combustion facility. This facility uses a neon-cooled cryomagnet capable of producing magnetic fields in excess of 5 tesla. The effects of power takeoff location, generator loading, B-field strength, and electrode breakdown on generator performance are discussed. The experimental data is compared to a theory based on one-dimensional flow with heat transfer, friction, and voltage drops.

I. Introduction

Combustion driven magnetohydrodynamic (MHD) generators show great promise for both flight and ground-based electrical power generation. The Lewis Research Center (LeRC) has in operation a small (4-12 MW_T) cesium-seeded H_2-O_2 combustion MHD generator to investigate performance and fluid dynamics at high magnetic field levels. This combustion system was chosen because of its attractiveness for lightweight systems, the H_2-O_2 combustion expertise at LeRC, and the simplicity of the H_2-O_2 system which facilitates the understanding of the basic processes involved.

The MHD power generation experiments are conducted in a high magnetic field strength cryomagnetic facility. While this facility has the capability to produce fields >6 tesla, the peak field utilized to date is 5 tesla. In the initial experiments, the Hall generator configuration was chosen for its simplicity of construction and is designed to operate supersonically (Mach 2 at entrance) over a range of combustion pressures (5-20 atm) and a range of oxygen/fuel weight ratios (4-12). This facility and the associated MHD hardware are discussed in Section II.

In experiments carried out to date, the effects of power takeoff location, generator loading, B-field strength, and electrode breakdown voltage have been investigated. It is found that the maximum power output for our present experimental configuration with a single load occurs with the front power leads located approximately one-third of the distance downstream from the entrance of the generator. Effects of generator loading and B-field strength indicate that the overall internal resistance of the Hall generator only weakly depends upon B-field strength, and that the power output is proportional to the square of the B-field. Electrode breakdown is found to occur with arc damage to the anode wall. This breakdown occurs at interelectrode voltages in the range of 50 volts/insulator. These results are discussed in Section III.

In Section IV, a comparison between theory and experiment is presented. The theory is based upon one-dimensional flow with heat transfer, friction and voltage drops. The friction factor is determined empirically while the voltage drops are taken from previous experiments[1] performed under similar conditions. Reasonable agreement is obtained between theory and experiment for axial pressure data. The measured axial voltage profile is found to be in excellent agreement with theory at low magnetic fields (2.5 tesla), but the theory tends to underestimate the voltage at higher fields (4.5 tesla).

II. Experimental Facility

The MHD power generation experiments are conducted in a high field strength cryomagnet (fig. 1) which was adapted from an existing facility. In its original construction, it consisted of 12 high purity aluminum coils pool cooled in a bath of liquid neon. In this configuration, a peak field of 15 tesla was produced. For the present experiments, the center four coils were removed and a 23 cm diameter transverse warm bore tube was inserted to allow the placement of the MHD experiment between the remaining eight coils as shown in the cross section insert in Figure 1. In this configuration, a peak field of >6 tesla should be obtainable. The time duration of the experiment is limited by the neon supply which allows on the order of 1 minute of total operating time followed by an 18-hour reliquefaction period. As a result, the experiments are run in a pulsed mode. The run duration for the data presented here was 5 sec. The magnetic field profile along the MHD duct is shown in Figure 2.

In the rocket engine modified for use in this program, the gaseous H_2 is injected uniformally into the combustion chamber through a porous stainless steel injection plate at the rear of the chamber. The gaseous O_2 is injected through 36 injection tubes uniformally inserted into the H_2 injection plate. Cesium seed is injected into the oxygen supply line as a 75% solution of CSOH dissolved in water. The combustion chamber and nozzle are water-cooled electrodeposited copper capable of steady-state operation. The length of the chamber and nozzle is 22.86 cm and the i.d. for the chamber is 6.35 cm. The nozzle is designed for Mach 2 at the 4.96 cm diameter exit. The engine is capable of operation at stagnation pressures between 5 and 20 atm and at O/F weight ratios from 4-12.

Initial experiments have been carried out using a diverging circular cross section duct having an inlet Mach number of 2 and an exit to inlet area ratio of 2.56. The heat sink duct is constructed from 42 copper electrodes, 1.27 cm wide and electrically insulated from one another by a high temperature asbestos sheet (to provide pressure seal), sandwiched between two sheets of mica (to provide electrical insulation). The duct (fig. 3) is built up in modular form, each module consisting of 8-15.24 cm o.d. rings clamped together between two triangular shaped pieces by three electrically insulated stainless

steel bolts. Lateral movement of the rings is negated by three fiberglas rods inserted through the entire module. As shown in Figure 2, four such modules are used in the present experiments with 2.54 cm end flanges for a total of 42 electrodes. Figure 3 is a picture of the combustor-generator-diffuser assembly.

The entire combustor-generator-diffuser assembly is inserted in the bore tube as shown in Figure 1. The high temperature exhaust gases are water quenched at the exit of the diffuser. The resulting water then passes back to a sump for recirculation. The water is periodically brought back to normal PH by acid addition after which it can be discarded through storm sewers.

While the facility is capable of being run over a wide range of parameters, the data which will be discussed in this report was taken for the following nominal conditions:

Combustion stagnation pressure	≈10 atm
Mass flow rate	≈0.5 kg/sec
Seed fraction $\equiv \frac{\text{wt. of Cs}}{\text{tot. wt.}}$	≈0.05
Equivalence ratio	≈1.0
Thermal input	≈7 MW
Peak magnetic field	≈5 tesla
Entrance Mach number	≈2
Duct entrance diameter	≈5.0 cm
Duct exit diameter	≈8.0 cm
Length of duct	≈58 cm

III. Experimental Results

Effect of Power Takeoff Location

In these initial experiments, the Hall generator configuration was chosen over the more efficient Faraday or diagonal wall configurations due to its simplicity of construction. One advantage of the Hall and DW configurations over that of the Faraday is that power can be extracted by a single electrical load rather than requiring separate loads for each electrode. However, this can be a disadvantage since as the gas properties (particularly the electrical conductivity) change down the channel, the axially varying local internal impedance cannot be matched by the single external impedance.

The result of this is shown in Figure 4. In this figure the generated voltage is plotted as a function of distance down the channel, i.e., electrode number. In Run 407, the external load (11.5 Ω) was placed between the first three and the last three electrodes. It is seen that the voltage gradient between the third and twelfth electrode is negative indicating that power is being dissipated in this region. This is due to the fact that insufficient voltage is being generated in this region to pass the current generated by the generator as a whole.

By eliminating this region from the load, i.e., moving the front power takeoff from electrodes 1-3 to electrodes 10-16, the power output was increased from 8.74 kW in Run 407 to 11.2 kW in Run 413. It should also be noted that in Run 413 the voltage gradient between electrodes 1-10 is now positive, and hence additional power could be obtained from this region by loading it with an appropriately matched impedance. The multiple loading of Hall generators to obtain more optimal performance will be considered in future experiments. In the experimental data to be discussed in the following sections, the power takeoff electrodes were 11-13 to 40-42.

Effect of External Loading and B-Field

Figure 5 shows the loading diagram for the MHD generator at various magnetic field strengths. The scatter in the data is shown by the error bars about the circled point which is the average. The surprising result of this plot is the relative independence of the internal impedance as measured by the slope of the curves upon magnetic field. The internal impedance as measured in this manner is plotted in Figure 6 as a function of magnetic field strength. It is seen that the dependence is weak which is not what one would expect from the theoretical relation for a Hall generator

$$R \sim \int_0^{\ell} \frac{1+\beta^2}{\sigma A}\, dx \qquad (1)$$

where R is the internal impedance, ℓ is the length of the power generating region, β is the Hall parameter, σ is the electrical conductivity, and A is the duct cross sectional area.

For the conditions of the present experiments, β is in the range 1-2 and hence one would expect that R would be sensitive to the magnetic field strength. However, theoretical calculations indicate that the $\underline{j} \times \underline{B}$ force is of sufficient magnitude so as to slow the plasma down to a degree that causes the temperature to increase in the power generation region. This results in an increase in σ which compensates to a large degree for the increase in $1 + \beta^2$.

Power Output

In Figure 7 the effect of B-field on the power generated is shown. It is seen that the power increases almost linearly with B^2. This dependency for a Hall generator at low Hall parameter (≈1) was not expected. Our initial theoretical analysis indicates that it is a result of axial variations in plasma parameters and the extreme sensitivity of our experiment to voltage drops due to the smallness of the device and the cold walls. These effects result in the B^2 dependency which is probably unique to our operating conditions and experiment. The maximum power output to date is 87.5 kW.

In Figure 8 the power density as a function of distance down the channel is plotted for various B-fields. These curves were obtained by differentiating the measured Hall voltage profiles to obtain the local Hall electric field

and by assuming that the measured Hall current completely and uniformly fills the duct cross sectional area, so that the local current density could be obtained by dividing the measured current by the area. It is noted that at the low B-field strengths, the power density is nearly constant at the end of the duct indicating that sufficient B-field is still available to generate additional power by increasing the duct length.

At the higher magnetic field strengths the power density, however, peaks and then decreases with distance down the channel. This is due to the $\underline{j} \times \underline{B}$ interaction which at high B-fields is sufficient to slow the gas down to a degree that the generated voltage, i.e., $\underline{u} \times \underline{B}$, decreases. This indicates that higher power levels can be obtained by expanding the flow more to increase its velocity in the end region of the duct. This can be accomplished by increasing the area. The maximum peak power density achieved to date is ≈84 MW/M^3 at 5 tesla.

Voltage Breakdown

In the above experiments, no electrical breakdown was observed. However, the interelectrode stress did not exceed the normally accepted breakdown level of ≈40 volts/insulator. In order to determine if the H_2-O_2 combustion system would be limited by the same breakdown level, the generator was operated open circuit. In Figure 9, the open circuit Hall voltage is plotted versus the square of the magnetic field. During the duration of our 5 second runs, no breakdown is observed below an average field of approximately 50 volts/insulator. Above this value the voltage still continues to increase with B^2. However, approximately 2.5 seconds after initiation of seed injection, breakdown occurs. After breakdown, a steady average voltage of approximately 40 volts/insulator is observed independent of magnetic field strength.

Upon disassembly of the channel, grooves approximately one-sixteenth of an inch wide perpendicular to the magnetic field were found to exist on the interelectrode insulators on the anode side of the channel. The damage was typical of the insulator shown in the upper right-hand corner of Figure 10. The severity of the damage to the insulators (as measured by the length of the grooves) very nearly correlated to the power density profile shown in Figure 8. This effect was also observed in Ref. 1 and is due to the $\underline{j} \times \underline{B}$ force acting on the anode current tending to force it into the insulators.

At this point, the duct had approximately 20 minutes of test time on it. In order to determine if the observed insulator damage was due solely to breakdown or just to general deterioration, the channel was rebuilt with new insulators. In the next series of tests, the duct was operated in the breakdown region with breakdown being observed on approximately one-third of the test runs. After approximately 2.4 minutes of test time, CSOH/H_2O leakage was observed through an electrode insulator and the experiment was stopped. Inspection of the insulators showed the severe damage as shown by the other three insulators in Figure 10. The channel was again rebuilt and operated below the breakdown region for an accumulative run time of 5.5 minutes with no observable damage to the insulators indicating that insulator damage was solely due to arc breakdown at the anodes.

IV. Theoretical Analysis

The primary purpose of the initial experiments is to verify our present theoretical codes and to provide confidence for their use as a design tool for future generator configurations. The present analysis is based upon a one-dimensional code taking into account friction and heat transfer. The MHD generator is modeled by considering the region between electrodes 1-11 to be an open-circuited Hall generator, the power takeoff regions between electrodes 11-13 and 40-42 to be a short-circuited Hall generator, and the region between electrodes 13-40 to be a normally loaded Hall generator. Since the code is one-dimensional, boundary layer effects must be accounted for by an empirical friction factor determined by experiment. This factor is determined by matching the axial pressure profile to the experimental data with no B-field, i.e., no electromagnetic interaction. In previous experiments[2], this factor was determined to be three times smooth pipe for our original flow train hardware. Modifications of the nozzle contour results in a value of 2.5 times smooth pipe in our present experiments. The agreement of this factor with experimental data is shown by the curve in Figure 11 for Run 460, i.e., 0 B-field.

The other parameter required by this theory is the electrode voltage drops. These drops result primarily from the passage of current through the cold boundary layers. They can be calculated by using the experimentally measured axial voltage profiles in the theory. However, at present the result obtained in experiments carried out in Germany[1] under similar conditions is being used. Their measurements indicated that while run-to-run variations did occur that, on the average, the voltage drop was:

$$V.D. = 100 + 50\ J$$

where J is the local Faraday current density in amp/cm^2.

Using the above parameters in the one-dimensional theory, the agreement with the experimental axial pressure data at 5 tesla is shown in Figure 11 for Run 480. It is seen that while the agreement with experiment is not exact, the theory predicts the general trend of the data. Comparison between theory and experiment for the axial Hall voltage profiles is shown in Figure 12. The theory provides excellent agreement with experiment at 2.5 tesla. However, the theoretical results at higher field strengths (4.5 tesla) tend to under predict the experimental results. Obviously, there is a B-field dependence in our experiments not observed in the German experiments which requires further investigation.

V. Concluding Remarks

In this paper the effects of power takeoff location, generator loading, magnetic field strength, and electrode breakdown voltage have been investigated in a Hall generator operating with a stoichiometric mixture of H_2-O_2 seeded with Cs (5% by weight). The entrance Mach number

is 2 and the combustion pressure is 10 atm. Still to be investigated are the effects of stoichiometry, combustion pressure and seed fraction on performance.

Initial experiments indicate that performance increases are possible by:

1. Increasing the duct length to utilize the low magnetic field region of the magnet.

2. Use multiple loads on the duct in order to obtain power output from the front of the duct.

3. Increasing the area in the rear of the duct to maintain the velocity which is slowed down by the $\underline{j} \times \underline{B}$ interaction at high B-field.

However, the initial results also indicate that further gains in peak performance may be limited by voltage breakdown since electric field strengths in the region of peak power output approach values at which breakdown was observed in open circuit operation. In order to circumvent this, multiple loading may be required so that the peak region can be operated off optimum load (toward short circuit) to reduce the electrical stress while the rest of the generator is allowed to operate at optimum load. Also to be investigated is the use of finer segmentation in the region of high electrical stress.

VI. References

1. Zankl, G., et al.: Experimental Determination of Design Data for an MHD Generator. Proceedings of the Thirteenth Symposium on the Engineering Aspects of Magnetohydrodynamics. Stanford University, 1973, pp. II.6.1-II.6.7.

2. Smith, J. M.: Results and Progress on the NASA Lewis H_2-O_2 MHD Program. Proceedings of the Fifteenth Symposium on the Engineering Aspects of Magnetohydrodynamics. University of Pennsylvania, 1976, pp. IX.2.1-IX.2.6.

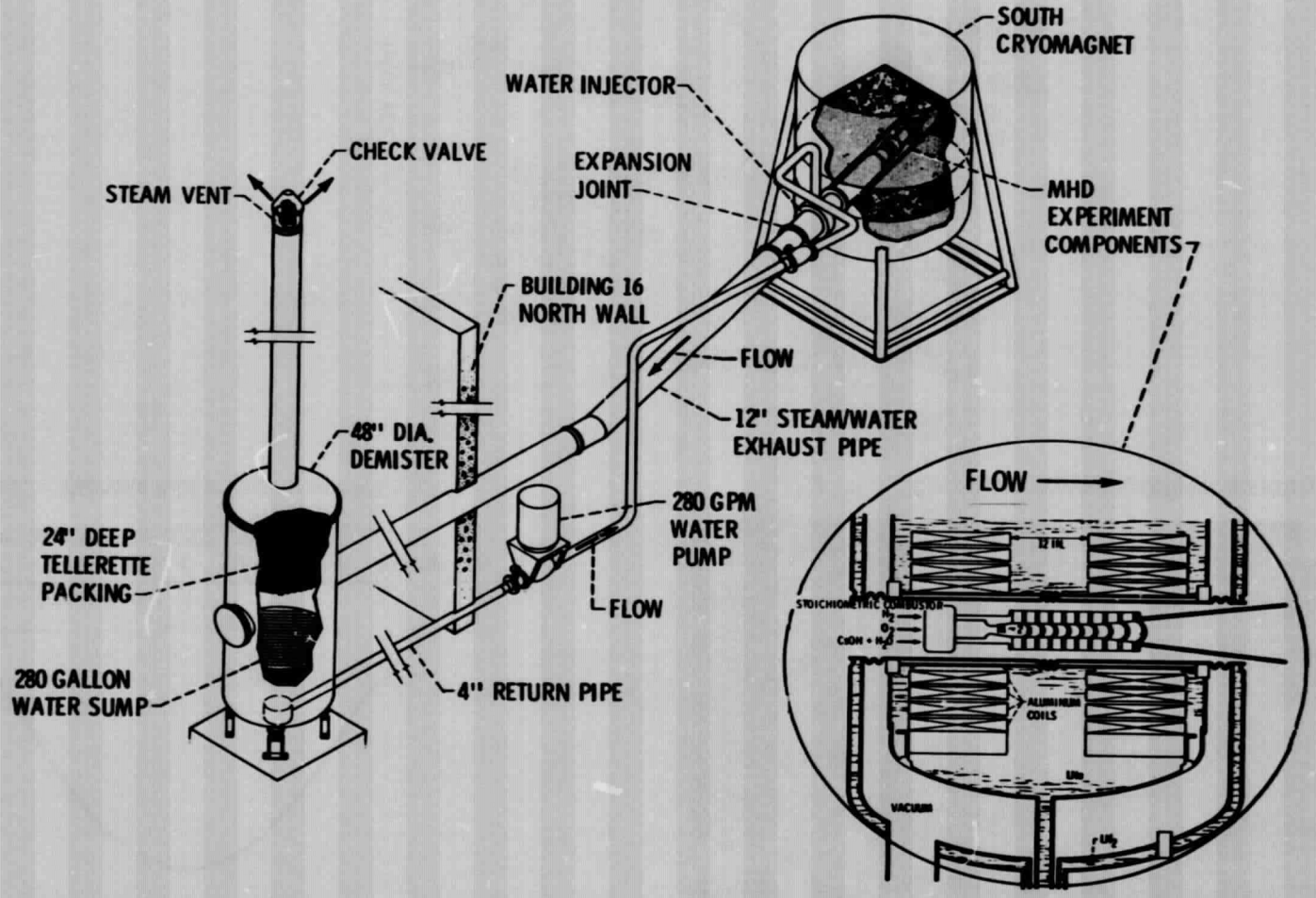

Figure 1. - GH_2-GO_2 combustion MHD experiment installation building 16 room 160.

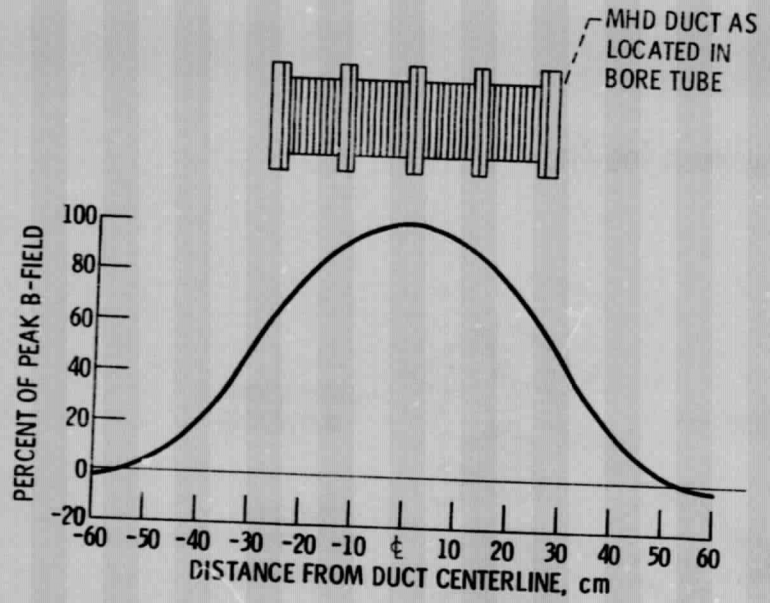

Figure 2. - Magnetic field profile along MHD duct.

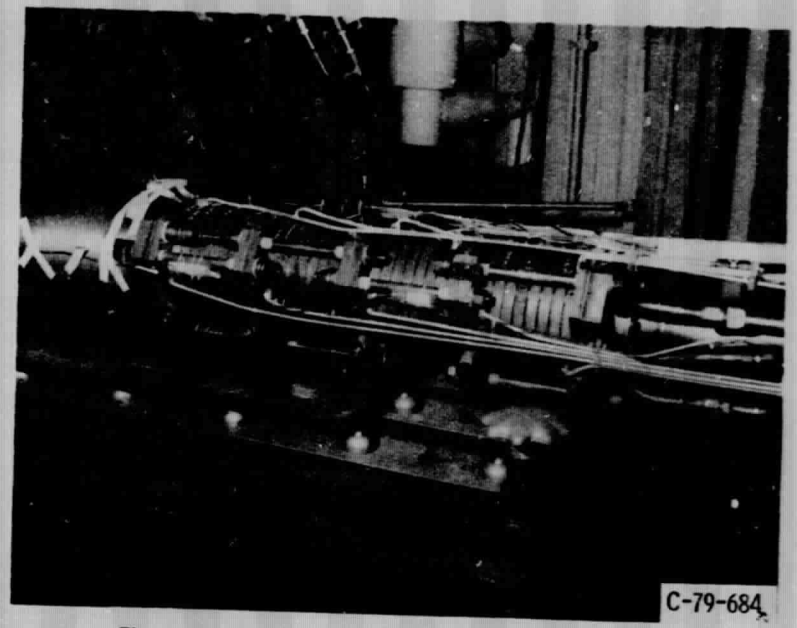

Figure 3. - Combustor-generator-diffuser assembly.

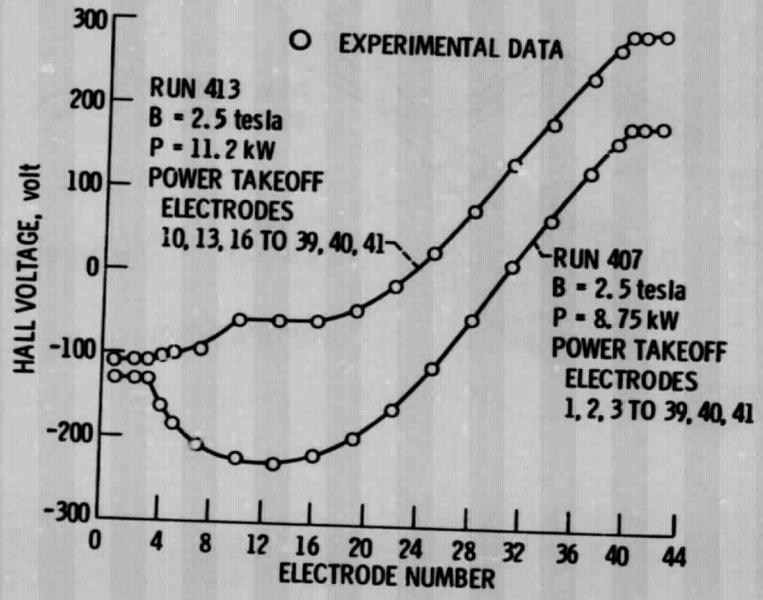

Figure 4. - Effect of electrical load on generator performance.

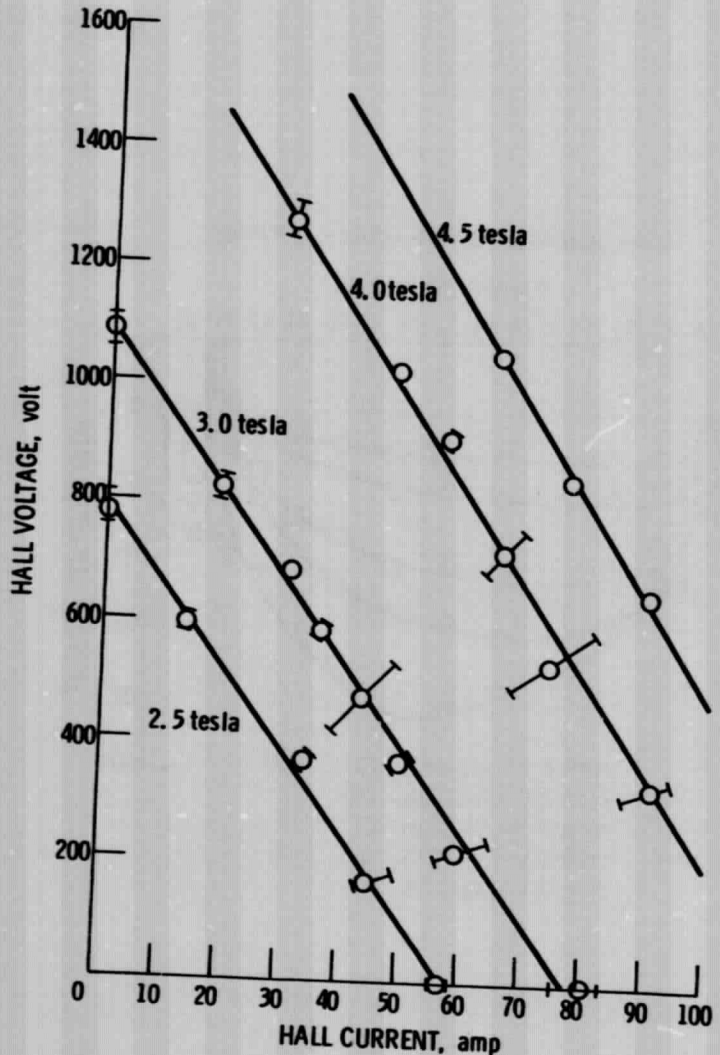

Figure 5. - MHD generator load curve. Power takeoff electrodes 11-13 to 40-42.

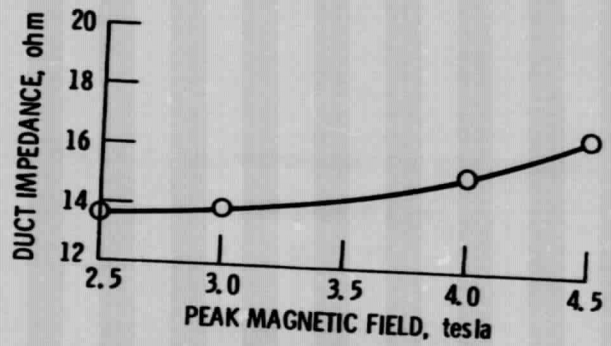

Figure 6. - Duct impedance as function of magnetic field strength.

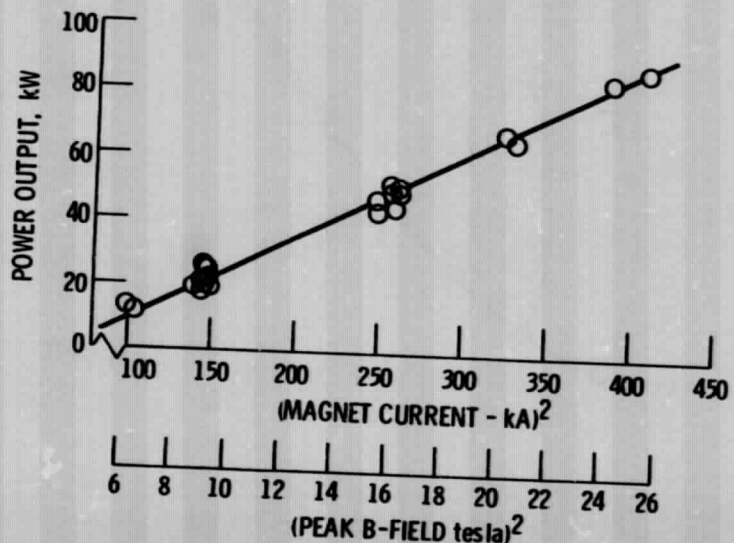

Figure 7. - Power output versus B^2.

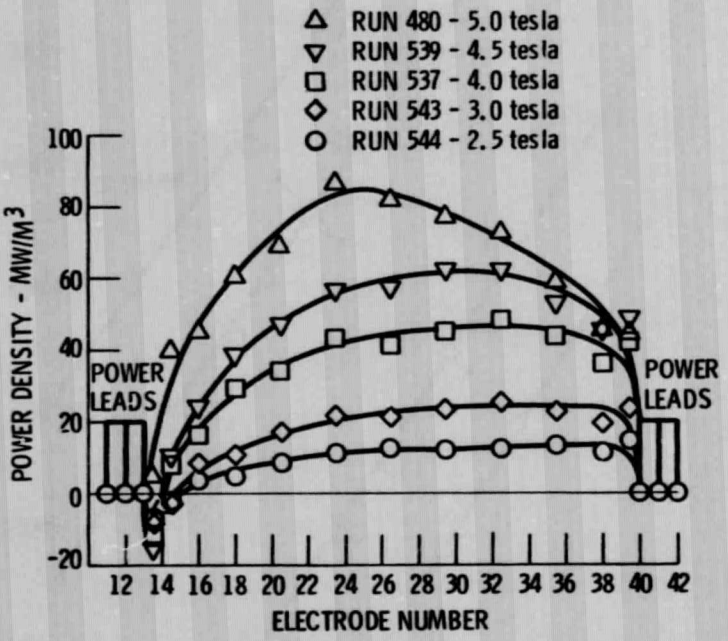

Figure 8. - Power density along MHD duct.

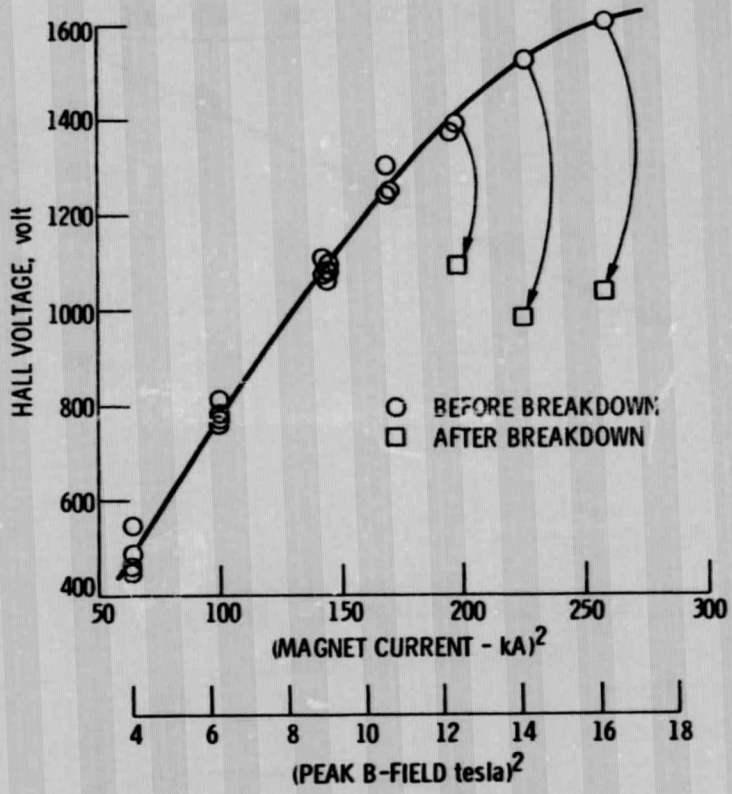

Figure 9. - Hall voltage before and after breakdown.

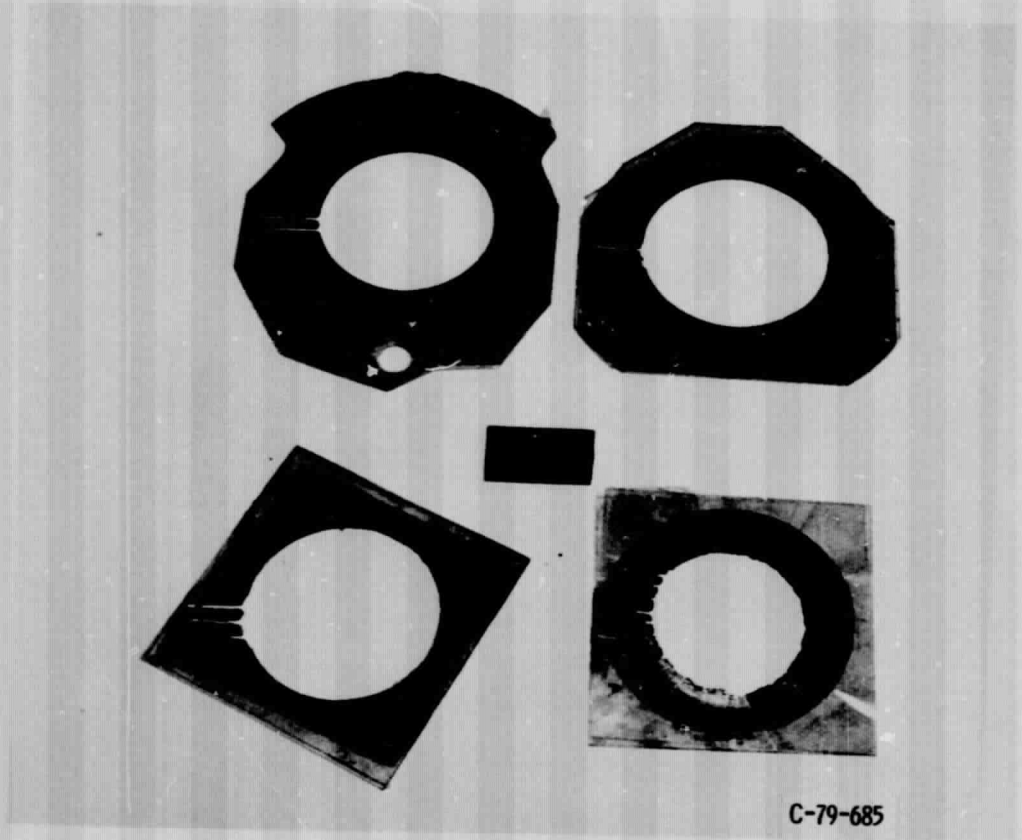

Figure 10. - Interelectrode insulator damage.

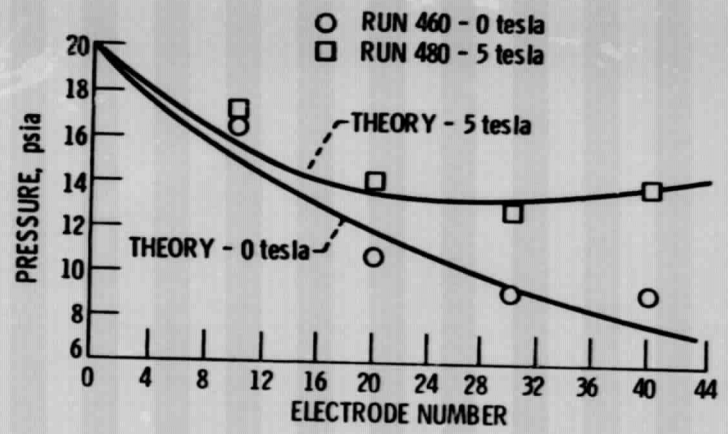

Figure 11. - Axial pressure profile.

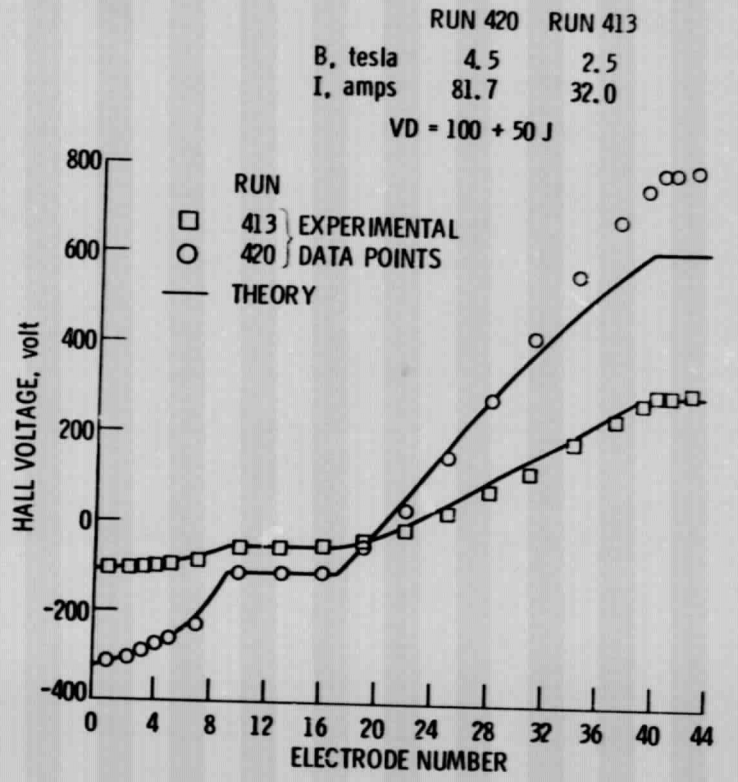

Figure 12. - Comparison between theory and experiment.